



A First Spectroscopic Measurement of the Magnetic-field Strength for an Active Region of the Solar Corona

Ran Si^{1,2} , Tomas Brage¹ , Wenxian Li^{1,3} , Jon Grumer⁴ , Meichun Li^{5,6}, and Roger Hutton⁵ 

¹ Division of Mathematical Physics, Department of Physics, Lund University, SE-221 00 Lund, Sweden; tomas.brage@fysik.lu.se

² Spectroscopy, Quantum Chemistry and Atmospheric Remote Sensing (SQUARES), CP160/09, Université libre de Bruxelles, Av.F.D. Roosevelt 50, B-1050 Brussels, Belgium

³ Department of Materials Science and Applied Mathematics, Malmö University, SE-20506 Malmö, Sweden

⁴ Theoretical Astrophysics, Department of Physics and Astronomy, Uppsala University, Box 516, SE-751 20 Uppsala, Sweden

⁵ Shanghai EBIT Laboratory, Key Laboratory of Nuclear Physics and Ion-beam Application, Institute of Modern Physics, Department of Nuclear Science and Technology, Fudan University, 200433 Shanghai, People's Republic of China; rhutton@fudan.edu.cn

⁶ School of Electronic Information and Electrical Engineering, Huizhou University, 516007 Huizhou, People's Republic of China

Received 2020 May 11; revised 2020 June 24; accepted 2020 June 30; published 2020 July 29

Abstract

For all involved in astronomy, the importance of monitoring and determining astrophysical magnetic-field strengths is clear. It is also a well-known fact that the corona magnetic fields play an important part in the origin of solar flares and the variations of space weather. However, after many years of solar corona studies, there is still no direct and continuous way to measure and monitor the solar magnetic-field strength. We present here a scheme that allows such a measurement, based on a careful study of an exotic class of atomic transitions, known as magnetic induced transitions, in Fe^{9+} . In this contribution we present a first application of this methodology and determine a value of the coronal field strength using the spectroscopic data from Hinode.

Unified Astronomy Thesaurus concepts: [Active sun \(18\)](#); [The Sun \(1693\)](#); [Solar magnetic fields \(1503\)](#); [Solar corona \(1483\)](#); [Spectroscopy \(1558\)](#); [Atomic spectroscopy \(2099\)](#); [Astronomical techniques \(1684\)](#)

1. Introduction

Magnetic fields hold a central position within solar research; continuous or on-demand measurements of the magnetic fields in the solar corona remain one of the major challenges in solar physics (Casini et al. 2017). It is important for the prediction of solar events such as flares or coronal mass ejections and, ultimately, for space-weather forecasting to avert damage to navigation and communication satellites, interference with airplane navigation systems, and disruptions in power grids that could cause large-scale blackouts (Schrijver et al. 2015). Due to the potential threat to society and human well-being from variations in the space weather, it is important to develop methods to continuously monitor the magnetic fields of the corona and measure their strengths. The very recent inauguration of NSF's DKIST (Tritschler et al. 2016) and the launchings of the NASA mission Parker Solar Probe (launched in 2018 August) and the ESA/NASA mission Solar Orbiter (launched in 2020 February) observatories are forming an unprecedented solar corona and inner heliospheric campaign targeted at understanding how stars create and control their magnetic environments (Martinez Pillet et al. 2020). Unfortunately, a candidate for such a measurement has eluded the solar physics community. This may be the largest single factor blocking progress in coronal physics and is hindering the attempts to answer questions related to coronal heating, the triggering of flares, and coronal mass ejections, as well as the acceleration of the fast and slow solar wind (Solanki et al. 2006).

To address this, we have over the past few years been investigating a spectroscopic method based on quantum-interference effects in the Fe^{9+} ion (Li et al. 2015, 2016; Judge et al. 2016; Si et al. 2020). This particular interference is caused by magnetic fields external to the ion, and hence this idea has the potential to act as a probe of the coronal field strengths. In

this contribution we present a first application of this methodology and determine the values of the coronal field strengths using preexisting spectroscopic data from the Extreme-Ultraviolet Imaging Spectrometer (EIS) on the Hinode satellite (Culhane et al. 2007; Brown et al. 2008). The measurement is even fast enough, relative to the lifetime of solar flares, that we could track the development of the field as the flare develops.

Observing a single spectral line from an element in a certain charge state provides little information about the environment in which it was emitted, while a group of lines can give us a much more detailed picture. Just to give an example on how two lines can be used, their intensity ratio—especially if close in wavelength and from a single atomic charge state—often acts as a probe of the local electron density and temperature in the plasma (Feldman et al. 1978). To determine local plasma properties, the strategy is therefore reduced to finding a pair of lines of similar wavelength, where one originates from an upper level with a radiative decay rate of the same order of magnitude as the electron collisional de-excitation rate. The other line, which we will refer to as the normalization line, should have a radiative decay rate that is significantly faster and therefore its decay rate is insensitive to the collisional rates.

The same principle, where the intensity of one spectral line is sensitive and one insensitive to a certain environmental variable, can be used to measure other plasma properties. In this Letter we will discuss the strength of the magnetic field local to the observed ions and how it can induce new lines, the so-called magnetic-field induced transitions (MITs). It has been illustrated that the intensity of these lines can show a strong, to first order, quadratic dependence on the external field strength (Grumer et al. 2014). Since the magnetic fields inside the ions are enormous (in the ions of interest here on the order of hundreds or even thousands of Tesla), it requires, in the general case, strong external fields to induce these lines from

perturbations of the atomic structure. As an example, in Ne-like ions and for field strengths of a few Tesla, MITs have been observed using an electron beam ion trap (Beiersdorfer et al. 2003, 2016). Such cases are not of particular interest in solar physics, since the strongest fields we can observe are in a sunspot, and they are always weaker than 1 T.

The rate, and therefore the intensity, of an MIT of electric dipole (E1) type is to first order given by

$$A_{\text{MIT}} \propto A_{\text{E1}} \frac{B^2}{(\Delta E)^2}, \quad (1)$$

where B is the strength of the external magnetic field, ΔE is the energy separation between a metastable level and a nearby upper level of a fast E1 transition, in the following referred to as the feeding level, while A_{E1} is the decay rate of the feeding level. The metastable and feeding levels are mixed in the presence of an external magnetic field, which causes them to share their properties. This leads to the emergence of a new radiative transition from the metastable level, the MIT. Therefore, if one can find a metastable level that is close to a short-lived one in an abundant atomic charge state, one can expect that MITs could be observed in the presence of a magnetic field. Of particular interest are those cases where this energy separation is small enough to cause a pseudo-degeneracy, which leads to a dramatic increase in the MIT rate of Equation (1) and thus also in the sensitivity of the rate to the magnetic field. Such degeneracies are however not necessarily predicted by the symmetries and the gross structure model of the ion, but could instead occur by chance as a result of a rather complex atomic structure.

A search for an atomic system involving a suitable pseudo-degeneracy was initiated a few years ago (Li et al. 2015, 2016; Judge et al. 2016; Si et al. 2020), motivated by its potential as a magnetic-field probe. This led to the discovery of Fe^{9+} where the excited levels $3p^4 3d \ ^4D_{5/2}$ and $\ ^4D_{7/2}$ fulfill the requirements of being very close in energy and having significantly different lifetimes. Fortunately, for astrophysical applications, this pseudo-degeneracy exists in an iron ion with a large abundance in many celestial objects, among them the Sun. It was found that this system could give rise to a considerable MIT even for field strengths of the same order of magnitude as one might expect in the solar corona, which presently are inaccessible from direct measurements. This motivated further studies of the Fe^{9+} system and investigations of its potential as a probe of coronal magnetic fields. However, the pseudo-degeneracy of $\ ^4D_{5/2,7/2}$ makes the two lines to the ground state a challenge to resolve since the transitions are in the VUV region, whereas the energy difference is only around 3.6 cm^{-1} ; to move to an actual determination of the coronal field this method had to be refined and supported by complex atomic and solar models. In this Letter we can finally, for the first time, present a direct determination of these field strengths.

2. Modeling and Analysis

For the spectral modeling we use the CHIANTI-PY spectral synthesis code, which is tailored for interpretation of spectra from high-temperature, optically thin astrophysical sources, together with electron collision data from the Chianti database (Dere et al. 1997; Landi et al. 2013) and radiative transition data from Wang et al. (2020).

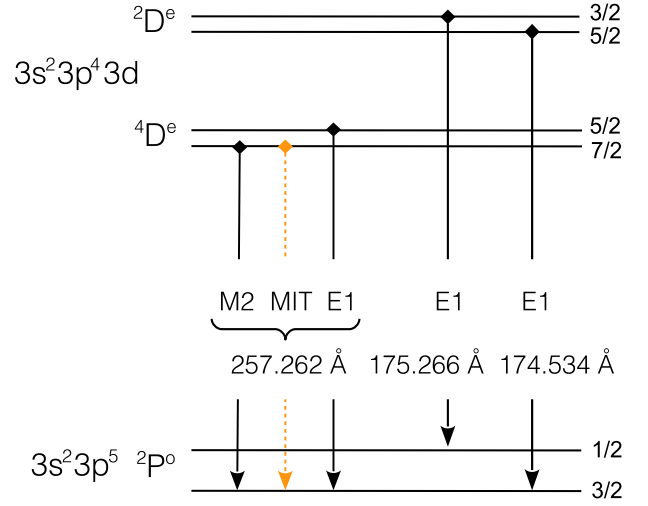


Figure 1. Schematic energy diagram and decay channels for the levels of Fe^{9+} that are relevant to the method discussed in this work (see the text). Wavelengths are given in \AA .

A partial energy level diagram of Fe^{9+} is shown in Figure 1, illustrating the levels and transitions of interest in this work. The synthetic Gaussian fitted spectra recorded by EIS on the Hinode satellite (Culhane et al. 2007; Brown et al. 2008) nearby the present lines of interest are shown in Figure 2 and demonstrate the lines in Figure 1 are well resolved by EIS. The main feature for this project is a blended group of three lines marked as having a wavelength of 257.262 \AA (denoted by E1, M2, and MIT in Figure 1). These are from two different upper levels, one being the $3s^2 3p^4 3d \ ^4D_{5/2}$ decaying to the ground level $3s^2 3p^5 \ ^2P_{3/2}^o$ through a so-called E1 spin-induced transition. This level represents the feeding level in our model. The other upper level is the $3s^2 3p^4 3d \ ^4D_{7/2}$ level, with a decay dominated by a forbidden M2 decay, in the absence of external magnetic fields, with a low transition rate. Finally, due to the very near energy degeneracy ($\Delta E \approx 0$) of this level with the $\ ^4D_{5/2}$ level, an external magnetic field induces a mixing of these two levels causing a magnetic-field induced E1 transition to the $\ ^2P_{3/2}^o$ ground level. For the important ΔE parameter introduced in Equation (1) we use the value of 3.6 cm^{-1} from the most accurate determination to date (Judge et al. 2016). The two transition rates required to model the MIT spectral line are (Wang et al. 2020)

$$A_{\text{E1}}(^4D_{5/2} \rightarrow ^2P_{3/2}^o) = 6.01 \times 10^6 \text{ s}^{-1}, \quad (2)$$

$$A_{\text{M2}}(^4D_{7/2} \rightarrow ^2P_{3/2}^o) = 5.78 \times 10^1 \text{ s}^{-1}. \quad (3)$$

As pointed out above, in the presence of a magnetic field, the metastable and feeding levels will interact, which is represented by the mixed state

$$|{}^4D_{7/2}^e\rangle = c_1|7/2\rangle + c_2|5/2\rangle, \quad (4)$$

where $J = 7/2$ and $5/2$ is the quantum number representing the total angular momentum of the ion, in a field-free space. The mixing coefficients, c_1 and c_2 , are obtained by determining and diagonalizing the interaction matrix for different magnetic fields, using the GRASP atomic structure suite of programs (Jönsson et al. 2013; Fischer et al. 2019, 2016) together with the HFSZEEMAN add-on module (Andersson & Jönsson 2008; Li et al. 2020). The $(B/\Delta E)^2$ proportionality of Equation (1) is

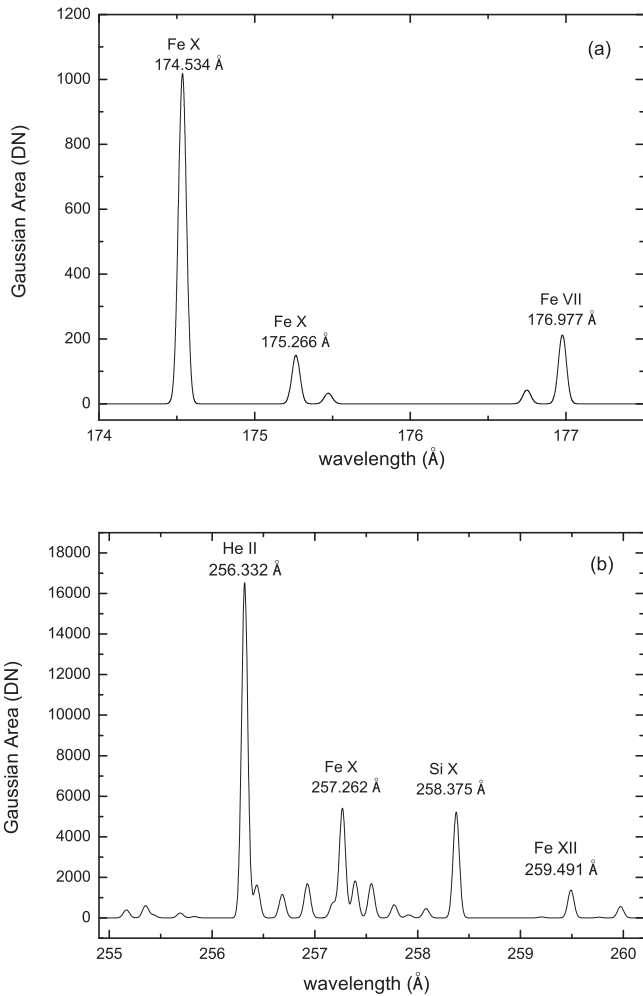


Figure 2. Synthetic Gaussian fitted spectra from the EIS short wave band (a) and long wave band (b) nearby the 257 MIT line (bottom panel) and reference lines (top panel) shown in Figure 1 for AR2. FWHM = 0.06 Å for the short wave band and FWHM = 0.07 Å for the long wave band, as recommended in Brown et al. (2008).

due to the c_2 mixing coefficient, since an estimated value for the rate in first-order representation can be written as

$$A_{\text{MIT}}(4D_{7/2} \rightarrow 2P_{3/2}^0) = |c_2|^2 A_{\text{E1}}(4D_{5/2} \rightarrow 2P_{3/2}^0). \quad (5)$$

By adding this rate for a number of magnetic-field strengths to the M2 rate, we can predict the intensity ratio for the combined transition from the $4D_{7/2,5/2}$ levels to the normalization lines and compare it to the observed ratio from the Hinode data (Brown et al. 2008).

The decay of the metastable $4D_{7/2}$ level is dominated by slow M2 and MIT radiative channels resulting in a lifetime of the order of 10^{-2} s, implying that the blended spectral feature could be sensitive to the electron densities found in the corona. In order to evaluate these collisional effects, the proposed method thus also requires simultaneous determination of the local electron density. From the CHIANTI-PY line intensity modeling at the wavelength range 165–290 Å and electron density range 10^8 – 10^{10} cm $^{-3}$, we found that the 174.534 Å line ($3s^23p^43d^2D_{5/2}$ – $3s^23p^5^2P_{3/2}^0$ as shown in Figure 1) is the strongest at all densities, while the relative intensity of the 175.266 Å line ($3s^23p^43d^2D_{3/2}$ – $3s^23p^5^2P_{1/2}^0$) to the 174.534 Å line increases with the electron density. By

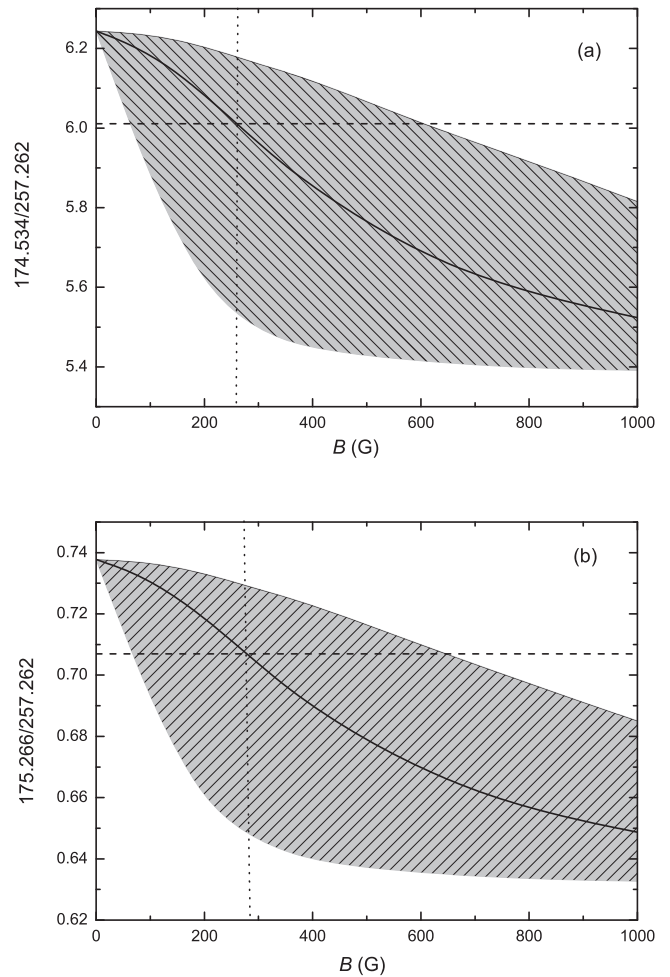


Figure 3. Simulated intensity ratio (black line) of (a) 174.534/257.262 and (b) 175.266/257.262 as a function of the magnetic field in the AR area. The gray shaded area shows the uncertainty caused by the uncertainty in the ΔE parameter (see the text). The horizontal dashed line is the line ratio measured from Hinode. The vertical dotted line shows our estimated magnetic strength.

adjusting the spectral model to simulate the measured intensity ratio, electron densities of 1.2×10^9 cm $^{-3}$ were established for one active region (AR2 in Brown et al. 2008). With these electron densities and the selected normalization lines 174.534 and 175.266 Å, magnetic-field strengths can finally be determined through comparisons of the spectral model with observed line ratios.

By combining theoretical modeling with the observation from Hinode, we estimate solar magnetic fields for AR2. Figure 3 present modeled line ratios as functions of magnetic-field strengths. Comparing with the observed line intensities from the active region, the best-fit magnetic fields only differ by about 4%, giving an estimated average field of $B_e = 270$ G from 265 and 275 G obtained from the line ratios with lines at 174.534 Å (Figure 3(a)) and 175.266 Å (Figure 3(b)), respectively. This is in accordance with previous estimations of 100–300 G based on extrapolation from magnetograms at the lower boundary, using a potential or force-free field model (Aschwanden 2014), which is not a direct measurement of the coronal magnetic fields.

There are a number of uncertainties to be considered, the dominating one coming from the determination of the fine structure energy (3.6 ± 2.7 cm $^{-1}$; Judge et al. 2016). The

shaded areas of Figure 3 show limits for the estimated magnetic fields due to the uncertainty in ΔE , with upper and lower boundaries at roughly $B_e/16$ and $3*B_e$, respectively. There are also possible uncertainties in the atomic data, especially in the M2 and the MIT rates. The MIT rate depends on the transition rate of the $^4D_{5/2}$, which is in itself a spin-forbidden transition to the $^2P_{3/2}^o$ ground state level. Theoretical determination of transition rates for spin-forbidden transitions have been improved considerably over the years, but it is hard to give an exact value of the uncertainty of this rate as no measurement of the $^4D_{5/2}$ rate for any ion in the Cl-like sequence is available (and this situation is not likely to change with the demise of beam-foil spectroscopy some years back; Träbert 2008). The estimated uncertainty of the present cited transition rate is $\leq 25\%$ (Wang et al. 2020), which will cause a maximum uncertainty of 12.5% in the estimated magnetic-field strengths. This is considerably smaller than the uncertainty introduced from the estimates of ΔE and can at the present stage of analyses be ignored. The M2 rate is easier to compute, but an added complication is that this decay component of the $^4D_{7/2}$ has a different angular dependence of its polarization pattern than the MIT (which is an electric dipole transition). One of the authors has investigated the magnetic-field-dependent angular distributions and linear polarization of E1, M2, and MIT transitions for the Ne-like ions (Li et al. 2014). When other error sources are reduced, it should be further investigated for Fe X, but we estimate it to be negligible compared to other sources of uncertainties in the present situation.

It is clear that the proposed method is a viable candidate for direct and continuous measurements of coronal fields. To outline a future space-based instrument designed from the proposed scheme, it would need a simple spectrometer isolating two narrow spectral regions, the short wavelength region covering the 174.543 and 175.266 Å lines, and a higher wavelength region for the 257.262 Å line. The spectrometer should be intensity calibrated, similarly to the present spectrometer on board Hinode. The other requirement that is of vital importance is the optimization of the signal-to-noise ratios. As can be seen in Figure 3(b), the AR area line ratio changes from 0.72 to 0.69 over a range of magnetic field from 200 to 400 G, i.e., a factor of 2 change in the field strength only results in a bit over 4% change in the line ratio. Therefore, the EIS LW–SW calibration and optimization of the signal-to-noise ratio are also critical factors for the success of this technique, although at the present stage the ΔE uncertainty is clearly the most important source of error.





3. Conclusion

We present for the first time direct, space-based measurements of the solar corona magnetic-field strength. The measurements are based on a magnetic-field-induced transition (MIT) in the spectrum of Fe^{9+} . So far, the MIT used here is the only one known to be sensitive to the relatively weak magnetic

fields found in astrophysical plasmas such as the solar corona. The field strength we determine is around 270 G. The most severe uncertainties come from the determination of the 4D fine structure and measured line intensities. Both of these are possible to improve in future work, by more accurate laboratory measurement (for the former) and an optimized design of a space-based observation (for the latter).

This work was supported by the Swedish Research Council (VR) under Contract No. 2015-04842 and the National Natural Science Foundation of China under Contract No. 11474069. J. G. would like to acknowledge financial support from the the project grants “The New Milky Way” (2013.0052) and “Probing charge- and mass-transfer reactions on the atomic level” (2018.0028) from the Knut and Alice Wallenberg Foundation. We also thank J. Leenaarts for helpful discussions.

ORCID iDs

Ran Si  <https://orcid.org/0000-0002-6206-4873>
 Tomas Brage  <https://orcid.org/0000-0003-3985-767X>
 Wenxian Li  <https://orcid.org/0000-0002-4569-1568>
 Jon Grumer  <https://orcid.org/0000-0002-6224-3492>
 Roger Hutton  <https://orcid.org/0000-0001-6558-2820>

References

- Andersson, M., & Jönsson, P. 2008, *CoPhC*, **178**, 156
 Aschwanden, M. J. 2014, in *Encyclopedia of the Solar System*, ed. T. Spohn, D. Breuer, & T. V. Johnson (3rd ed.; Boston, MA: Elsevier), 235
 Beiersdorfer, P., López-Urrutia, J. R. C., & Träbert, E. 2016, *ApJ*, **817**, 67
 Beiersdorfer, P., Scofield, J. H., & Osterheld, A. L. 2003, *PhRvL*, **90**, 235003
 Brown, C. M., Feldman, U., Seely, J. F., Korendyke, C. M., & Hara, H. 2008, *ApJS*, **176**, 511
 Casini, R., White, S. M., & Judge, P. G. 2017, *SSRv*, **210**, 145
 Culhane, J. L., Harra, L. K., James, A. M., et al. 2007, *SoPh*, **243**, 19
 Dere, K. P., Landi, E., Mason, H. E., Monsignori Fossi, B. C., & Young, P. R. 1997, *A&AS*, **125**, 149
 Feldman, U., Doschek, G. A., Mariska, J. T., Bhatia, A. K., & Mason, H. E. 1978, *ApJ*, **226**, 674
 Fischer, C. F., Gaigalas, G., Jönsson, P., & Bieroń, J. 2019, *CoPhC*, **237**, 184
 Fischer, C. F., Godefroid, M., Brage, T., Jönsson, P., & Gaigalas, G. 2016, *JPhB*, **49**, 182004
 Grumer, J., Brage, T., Andersson, M., et al. 2014, *PhyS*, **89**, 114002
 Jönsson, P., Gaigalas, G., Bieroń, J., Fischer, C. F., & Grant, I. 2013, *CoPhC*, **184**, 2197
 Judge, P. G., Hutton, R., Li, W., & Brage, T. 2016, *ApJ*, **833**, 185
 Landi, E., Young, P. R., Dere, K. P., Zanna, G. D., & Mason, H. E. 2013, *ApJ*, **763**, 86
 Li, J., Brage, T., Jönsson, P., & Yang, Y. 2014, *PhRvA*, **90**, 035404
 Li, W., Grumer, J., Brage, T., & Jönsson, P. 2020, *CoPhC*, **253**, 107211
 Li, W., Grumer, J., Yang, Y., et al. 2015, *ApJ*, **807**, 69
 Li, W., Yang, Y., Tu, B., et al. 2016, *ApJ*, **826**, 219
 Martinez Pillet, V., Tritschler, A., Harra, L., et al. 2020, arXiv:2004.08632
 Schrijver, C. J., Kauristie, K., Aylward, A. D., et al. 2015, *AdSpR*, **55**, 2745
 Si, R., Li, W., Brage, T., & Hutton, R. 2020, *JPhB*, **53**, 095002
 Solanki, S. K., Inhester, B., & Schüssler, M. 2006, *RPPH*, **69**, 563
 Träbert, E. 2008, *PhyS*, **78**, 038103
 Tritschler, A., Rimmele, T. R., Berukoff, S., et al. 2016, *AN*, **337**, 1064
 Wang, K., Jönsson, P., Zanna, G. D., et al. 2020, *ApJS*, **246**, 1